Avicenna J Environ Health Eng. 2018 Dec;5(2):115-119 http://ajehe.umsha.ac.ir

Original Article

doi 10.15171/ajehe.2018.15

Synthesis and Characterization of Ultrafine Ag/ZnO Nanotetrapods (AZNTP) for Environment Humidity Sensing

Babak Sadeghi*

Department of Chemistry, Tonekabon Branch, Islamic Azad University, Tonekabon, Iran

***Correspondence to**
Tel: +98 912 289 8500; Fax: +98 115 427 2484.
E-mail: b_sadeghi@toniau.ac.ir; bsadeghi1177@gmail.com

Published online December 29, 2018

Abstract
Ag/ZnO nanotetrapods (AZNTP) are prepared using silver (I)–bis (oxalato) zinc complex and 1, 3-diaminopropane (DAP) under a phase separation system. This crystal structure and lattice constant of the AZNTP was investigated by means of XRD, TEM, and UV-vis spectrum. AZNTP films with 23 nm in arm diameter and high surface activity work at room temperature as humidity sensors. AZNTP have shown some properties including quick response with high sensitivity, a longer life span and recovery, and no need for heat regeneration. Moreover, AZNTP could form OH group with physisorbed water in wet environments. The results of the present study demonstrated that the growth and characterization of AZNTP for environmental humidity sensing and DAP play an original role in the determination of particle morphology. Ultra-thin AZNTP has also been tested as a resistance sensor, having an unusual high sensitivity to moisture.

Keywords:1, 3-Diaminopropane (DAP), Ag/ZnO nanotetrapods (AZNTP), Bimetallic, Humidity sensors, Controlled growth, Transmission electron microscopy (TEM)

Received August 02 2018; **Revised** December 01, 2018; **Accepted** December 14, 2018

1. Introduction

Most humidity sensors are currently based on aluminum polymers and ceramic porous components in which a sensitive ionic humidification mechanism has been employed (1, 2). In the case of ceramics, due to water absorption (chemical and physical) and/or capillary density inside the cavities, it is necessary to react to oxides using the moisture by decreasing their impedance. This mechanism is done in low temperatures during which water should be on the surface of the phosphorus oxide (3-6). Various types of materials are used as humidity sensors, as well as sensors in commercial devices. In the meantime, ceramics have been used for their thermal and chemical stability and mechanical strength (7-11). However, each of these materials has its own limited uses. Different measurement mechanisms and operating principles have been identified for ceramic oxides using the variations in electrical parameters (12, 13). First, the detection of moisture depends on the processes of water absorption. The importance of these surface reactions for all these ceramic moisture sensors has been emphasized, as all of them are dependent on the level-related effects. High porosity and suitable surface area are favorable for increased sensitivity. The importance of particle size distribution in the electrical response to moisture from ceramic porous compounds is also mentioned (14-18). Other humidity sensors have recently been developed using various diagnostic mechanisms, from which high temperature moisture sensors from electrolytes use the electrolysis of high-voltage water vapor (>1.4 V). The electrolysis of adsorbed water is assumed to occur in contact sites with p-n. Therefore, p-n connections can be considered as another class of ceramic moisture sensors (19).

We have developed a reduction method of synthesis of Ag nanospheres and antibacterial activity (20), synthesized Ag/ZnO nanocomposites (21), and compared nanosilver particles and nanosilver plates for the oxidation of ascorbic acid (22, 23). Not only ZnO is a hydrophilic material that has been used for humidity detection (24), but also it has been ultra-thin Ag/ZnO nanotetrapods (AZNTP), which will lead to the conductivity of ZnO, dramatically and increasingly Indeed, the humidity sensors based on AZNTP have shown high sensitivity and recovery at room temperature. Due to Ultra-thin AZNTP, and double ionic layers in the inner wall of nanotertapods will lead to the conductivity of AZNTP dramatically and increasingly (25).

2. Materials and Methods

2.1. Materials

Zinc sulfide (silver) (I) -bis (oxalato) was synthesized. K_2ZnCl_4 (Merck, Germany) was dissolved in 20 mL of water, and 4 mM $K_2C_2O_4.H_2O$ (Sigma-Ald., Germany) Shaking was added at 55 ° C. In a little while, the solution turned orange and $K_2[Zn(C_2O_4)2].4H_2O$ was deposited. Then, 1.5 mM of $K_2[Zn(C_2O_4)_2]$, 1.5 mM of $AgNO_3$ and 1.5 mm of 1, 3 diaminopropane (DAP) was added to 20 mL of aqueous solution and shaken at 55°C and cooled in an ice water bath. In this process, $Ag_2[Zn(C_2O_4)2].3H_2O$ with yellow crystals were precipitated. After washing with cold water, yellow powder was stored in the dark. The nano alloys were formed slowly at the liquid/liquid interface and oxalate complex was found to prevent unfavorable silver halide formation and thus it was suitable for the formation of Ag/ZnO nanotetrapods (26, 27).

2.2. Characterization

The morphology and crystal structure of the co-deposited AZNTP were investigated by the Powder X-ray diffraction (XRD) pattern using the XD-3a quantum beam, and a nickel filter (λ = 1, 5418°C) was visible in an Argon 3003 PTC UV-Vis spectrum in the adsorption mode on the Hitachi U-2101 PC UV spectrophotometer. The sample solution was prepared by suspending a small amount of powder in the ethanol solution. At 100 kV, TEM was performed using a Philips EM208 microscope. After dispersing the powder in ethanol, samples were prepared. A few drops of suspension were coated in a 400 μkb grille with imaging carbon.

3. Results and Discussion

3.1. UV–Vis Spectral Studies

Absorption spectra were recorded for AZNTP with 17 nm in arm diameter after adding $ZnCl_2$ to AZNTP pre-prepared (as shown in Fig. 1). Surface plasmon resonance at about 410 nm was prepared and highlighted in AZNTP which showed that silver nanoparticles were formed separately. After Zn formation, amount of individual Ag nanoparticles is reduced, and then Zn covers the Ag nanoparticles (28, 29). After reducing $ZnCl_2$ (Ag formation), an increase in long-wave absorption was observed, showing the formation of larger objects like Tetrapod (30).

3.2. XRD and EDX

Figs. 2a and 2b show broad bands of the diffractograms of the bimetallic, while exhibiting sharp bands. The particle size is calculated based on the Scherrer equation:

$$t = \frac{0.9\lambda}{\beta \cos\theta} \quad (1)$$

where, t is the particle size in Å, λ is the X-ray wavelength, θ is the Bragg angle, and β corresponds to the full width at half maximum (FWHM, in radians) of the peak under consideration. As abovementioned, Ag/ZnO nanotetrapods (AZNTP) has values of d and 2θ, that are very close to each other (JCPDS 36- 1451, 4-0784). Fig. 2 (a and b) shows the XRD spectrums of the Ag/ZnO and AZNTP standard. While the Ag:Zn ratio was 1:1, the molecular weight of silicon to the metal was maintained at 100:5 level. XRD The spectrum of monosodium as well as bipolar from various compounds was recorded for samples prepared as dry powder (Fig. 2b). The courier, which appears at about 32 degrees (2θ), was related to the crystalline plate (100), and the peak was about 36◦ (2θ) related to the aircraft (101) (JCPDS 4-0784, 0681). While the plane (200) was less distinct (44.41◦), the diaphragmography showed that the crystallographic surface (111) was wide spread for silver clusters (38.46◦). Three additional band strips were observed at 57.48◦ (2θ), 62.48◦ (2θ), and 65.72◦ (2θ), respectively, corresponding

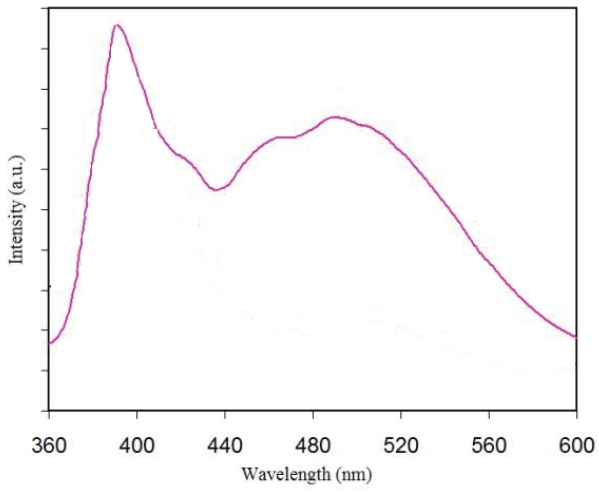

Fig. 1. UV-Spectra of Ag/ZnO Nanotetrapods (AZNTP) in Room Temperature With Mean Arm Diameter of 23 nm.

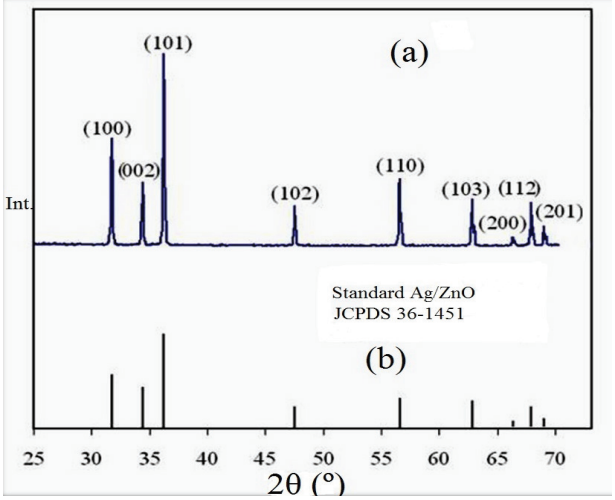

Fig. 2. XRD of Standard Ag/ZnO (a), and Ag/ZnO Nanotetrapods (AZNTP) Prepared (b). (JCPDS 36-1451).

to 110, 103, and 112 ZnO planes (29,30). This particle size (calculated using equation 1) was 25 ± 1 nm based on the peak (101). These values were near to the calculated values of the TEM measurements. An energy dispersive X-ray (EDX) spectrum of the AZNTP is shown in Fig. 3. Some features of Ag, Zn, and O atoms can only be observed in this spectrum. The appearance of Si peak in the spectrum was due to the substrate.

The detection of only Ag, Zn, and O atoms confirmed the preparation of AZNTP with high purity, although we could not deny the possible presence of some SiO_2 impurities which were not detectable in the XRD plot.

3. 3. TEM

The AZNTP dispersion had an arm diameter of 17–20 nm (Fig. 4); however, Ag nanoparticles were hardly discerned after ZnO- networked Ag colloids were formed. In the system where an aqueous 1 $\times 10^{-3}$ mol L^{-1} $AgNO_3$ solution was added to a ZnO nanoparticle dispersion 10 wt% formamide solution at ~100°C, core-shell of ZnO –Ag nanoparticles was formed which coexisted with AZNTP (Fig. 4).

For the AZNTP system, adding a small amount of Ag to ZnO (even a few percent) can affect the crystalline structure. As a result of the crystalline structure of Ag (31), it was suggested that coated nanoparticles are a solution composed of AZNTP, which is made up of a crystalline structure close to the silver, and released under heat treatment under internal stress, leading to solid solvent formation in the thermodynamic equilibrium. The change in the network parameter with thermal treatment was considered as the result of this building relaxation. The stable AZNTP observed in this study appears to be related to high energy levels for nanoscopic materials (32). Various features of this AZNTP such as magnetic transport and electron transport will be investigated.

3.4. Ag/Zno Nanotetrapods as Humidity Sensors

The humidity sensitivity is defined as:

$$S = \frac{I_{H2O} - I_{N2}}{I_{N2}}$$

where I_{H2O} is the current under a given relative humidity

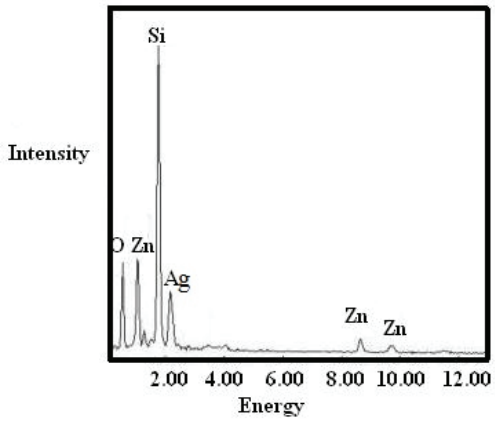

Fig. 3. EDX Spectrum Measured for Ag/ZnO Nanotetrapods (AZNTP) Prepared by the Zn and Ag Salts at 100 °C.

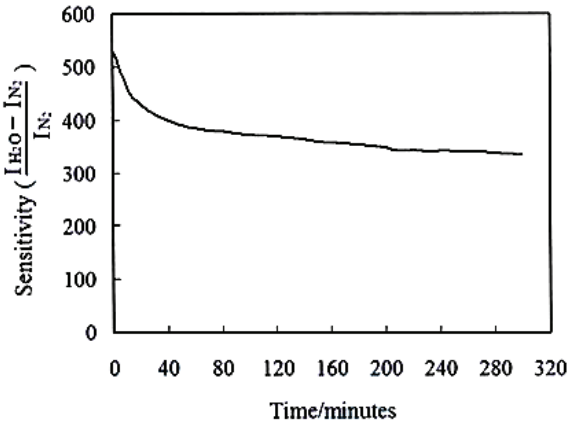

Fig. 5. Sensitivity Variation of the Ag/ZnO Nanotetrapods (23 nm in Arm Diameter).

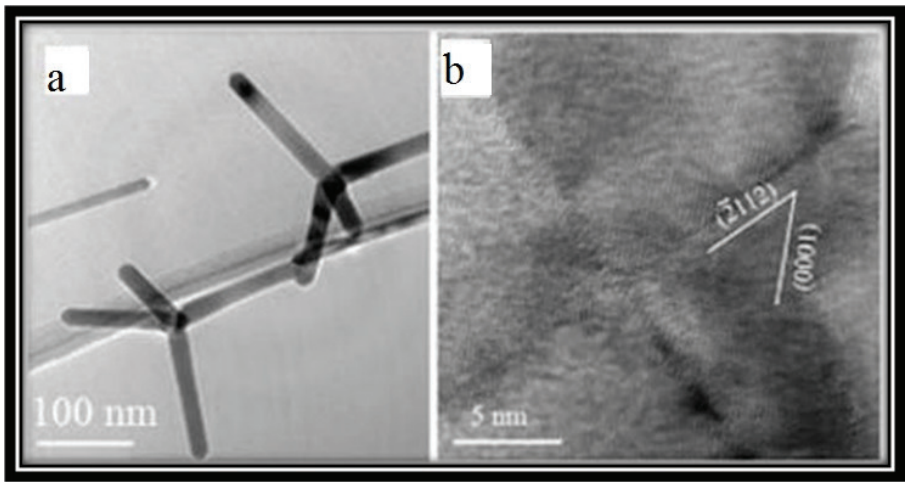

Fig. 4a-b. TEM Images of Ag/ZnO nanotetrapods (AZNTP) Prepared.

and I_{N2} is the current in pure nitrogen.

This sensor is made of AZNTP (22 nm in diameter). The sensitivity of AZNTP fewer than 100% relative humidity at 34ºC is about 335 and reproducibility is seen. The recovery and response are defined as reaching 96% and 4% maximum sensitivity which takes about 38 and 16 seconds, respectively. Fig. 5 shows the lifetime of AZNTP humidity sensor. We comparatively studied the humidity sensor performance between AZNTP of different sizes to demonstrate the virtue of AZNTP in relative humidity sensing (Fig. 6). In addition, due to larger surface area and available oxygen vacancies, small tetrapods (23 nm in arm diameter) were provided to be much more sensitive to humidity than larger tetrapods (80 nm in arm diameter) (33). According to the ionic-conduction mechanism, porosity and surface activity are two main factors in showing the humidity sensitivity of AZNTP.

This means that the capacitive component of the sensor impedance becomes more dominating at higher humidity (i.e. the transition frequency increases when the humidity level rises).

Thus, even when humidity increases, the resistive component of the sensor impedance remains dominant whilst the capacitive component of the sensor impedance becomes even less dominant. This result is a decrease of the transition frequency with increasing the humidity. For instance, the printed sensor head had a transition frequency around 75 kHz below 62% RH, but it reduced down to about 50 kHz above 77% RH. As a result, a printed sensor head, working between 155 kHz and 255 kHz, could always be considered as being primarily a resistive-type sensor.

4. Conclusion

In conclusion, the morphology, humidity sensor properties of the AZNTP were characterized. AZNTP has sensitivity to humidity and sensitivity increases with decreasing the size of tetrapod. The high sensitivity, quick response and recovery, high surface activity, and long lifetime of the tetrapods' humidity sensor with a stable OH group layer was formed and then covered with physisorbed water to wet environments. When tested as a resistance sensor, ultra-thin AZNTP also displays an unusual high sensitivity to moisture. This sensitivity increased significantly due to the specific level, but the more important reason was that it had two overlapping layers in the nanoscale channels, which caused a significant increase in the proton conduction. Humidity sensitivity has a certain level of good relationship with AZNTP with a diameter of 22 nm.

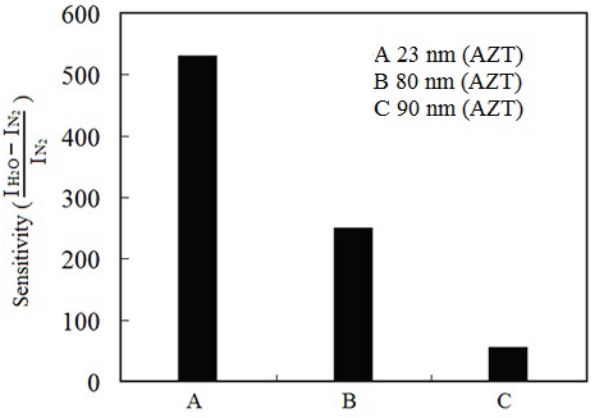

Fig. 6. Sensitivities of Different AZNTP Sensors at 34 °C. (A) AZNTP (23 nm in Arm Diameter); (B) AZNTP (80 nm in Arm Diameter); (C) AZNTP (90 nm in Arm Diameter). Note. The sensitivities of different AZNTP were comparatively studied under 60% and 100% relative humidity.

Acknowledgments

The financial support and encouragement was provided by the Research Vice-Presidency of Tonekabon Branch, Islamic Azad University.

References

1. Arai H, Seiyama T, Grpel W, Hesse J, Zemel JN. Sensors: A Comprehensive Survey. Weinheim VCH; 1992. p. 81-1012.
2. Ichinose N. Electronic Ceramics for Sensors. Am Ceram Soc Bull. 1985;64(12):1581-5.
3. Late DJ, Huang YK, Liu B, Acharya J, Shirodkar SN, Luo J, et al. Sensing behavior of atomically thin-layered MoS2 transistors. ACS Nano. 2013;7(6):4879-91. doi: 10.1021/nn400026u.
4. Late DJ, Kanawade RV, Kannan PK, Rout CS. Atomically thin WS2 nanosheets based gas sensor. Sens Lett. 2016;14(12):1249-54. doi: 10.1166/sl.2016.3764.
5. Late DJ. Liquid exfoliation of black phosphorus nanosheets and its application as humidity sensor. Microporous Mesoporous Mater. 2016;225:494-503. doi: 10.1016/j.micromeso.2016.01.031.
6. Erande MB, Pawar MS, Late DJ. Humidity sensing and photodetection behavior of electrochemically exfoliated atomically thin-layered black phosphorus nanosheets. ACS Appl Mater Interfaces. 2016;8(18):11548-56.
7. Tudorache F, Petrila I, Popa K, Catargiu AM. Electrical properties and humidity sensor characteristics of lead hydroxyapatite material. Appl Surf Sci. 2014;303:175-9. doi: 10.1016/j.apsusc.2014.02.138.
8. Zhang Y, Yu K, Jiang D, Zhu Z, Geng H, Luo L. Zinc oxide nanorod and nanowire for humidity sensor. Appl Surf Sci. 2005;242(1-2):212-7. doi: 10.1016/j.apsusc.2004.08.013.
9. Yuan Z, Tai H, Bao X, Liu C, Ye Z, Jiang Y. Enhanced humidity-sensing properties of novel graphene oxide/zinc oxide nanoparticles layered thin film QCM sensor. Mater Lett. 2016;174:28-31. doi: 10.1016/j.matlet.2016.01.122.
10. Abband Pashaki R, Sedigh Ziabari SA. Representation of the temperature nano-sensors via cylindrical gate-all-around Si-NW-FET. Int J Nano Dimens. 2015;6(4):377-83. doi: 10.7508/ijnd.2015.04.006.
11. Riazian M, Ramezani R. Low temperature formation Silver-Copper alloy nanoparticles using hydrogen plasma treatment for fabrication of humidity sensor. Int J Nano Dimens. 2013;3(4):297-301. doi: 10.7508/ijnd.2012.04.006.
12. Kulwicki BM. Ceramic materials based on perovskite-type oxides can be used as humidity sensors. J Am Ceram Soc. 1991;74(4):697-707.
13. Fagan JG, Amarakoon VRW. Reliability and reproducibility

of ceramic sensors: Part III. humidity sensors. Am Ceram Soc Bull. 1993;72(3):119-30.
14. Shimizu Y, Arai H, Seiyama T. Theoretical studies on the impedance-humidity characteristics of ceramic humidity sensors. Sens Actuators. 1985;7(1):11-22. doi: 10.1016/0250-6874(85)87002-5.
15. Sun HT, Wu MT, Ping L, Yao X. Porosity control of humidity-sensitive ceramics and theoretical model of humidity-sensitive characteristics. Sens Actuators. 1989;19(1):61-70. doi: 10.1016/0250-6874(89)87058-1.
16. Shimizu Y, Shimabukuro M, Arai H, Seiyama T. Humidity-Sensitive Characteristics of La3+-Doped and Undoped SrSnO3. J Electrochem Soc. 1989;136(4):1206-10.
17. Kim TY, Lee DH, Shim YC, Bu JU, Kim ST. Effects of alkaline oxide additives on the microstructure and humidity sensitivity of MgCr2O4-TiO2. Sens Actuators B Chem. 1992;9(3):221-5. doi: 10.1016/0925-4005(92)80220-R.
18. Gusmano G, Montesperelli G, Nunziante P, Traversa E. Microstructure and electrical properties of MgAl2O4 and MgFe2O4 spinel porous compacts for use in humidity sensors. Br Ceram Trans. 1993;92:104-108.
19. Yagi H, Ichikawa K. Humidity sensing characteristics of a limiting current type planar oxygen sensor for high temperatures. Sens Actuators B Chem. 1993;13(1-3):92-5. doi: 10.1016/0925-4005(93)85332-5.
20. Toyoshima Y, Miyayama M, Yanagida H, Koumoto K. Effect of relative humidity on current-voltage characteristics of Li-doped CuO/ZnO junction. Jpn J Appl Phys. 1983;22(12):1933. doi: 10.1143/jjap.22.1933.
21. Ushio Y, Miyayama M, Yanagida H. Fabrication of thin-film CuO/ZnO heterojunction and its humidity-sensing properties. Sens Actuators B Chem. 1993;12(2):135-9. doi: 10.1016/0925-4005(93)80009-Z.
22. Yanagida H. Intelligent ceramics. Ferroelectrics. 1990;102(1):251-7. doi: 10.1080/00150199008221485.
23. Sadeghi B. Green synthesis of silver nanoparticles using seed aqueous extract of Olea europaea. Int J Nano Dimens. 2014;5(6):575-81.
24. Wang XH, Ding YF, Zhang J, Zhu ZQ, You SZ, Chen SQ, et al. Humidity sensitive properties of ZnO nanotetrapods investigated by a quartz crystal microbalance. Sens Actuators B Chem. 2006;115(1):421-7. doi: 10.1016/j.snb.2005.10.005.
25. Sadeghi B, Rostami A, Momeni SS. Facile green synthesis of silver nanoparticles using seed aqueous extract of Pistacia atlantica and its antibacterial activity. Spectrochim Acta A Mol Biomol Spectrosc. 2015;134:326-32. doi: 10.1016/j.saa.2014.05.078.
26. Coucouvanis D, Piltingsrud D. Metal complexes as ligands. III. Bonding interactions of the anionic metal dithiooxalate complexes with the coordinately unsaturated bis (triphenylphosphine) copper (I) and bis (triphenylphosphine) silver (I) complex cations. J Am Chem Soc. 1973;95(17):5556-63.
27. Macintyre JE. Dictionary of inorganic compounds. 1st ed. London: Chapman & Hall; 1992.
28. Link S, El-Sayed MA. Spectral properties and relaxation dynamics of surface plasmon electronic oscillations in gold and silver nanodots and nanorods. J Phys Chem B. 1999;103(40):8410-26. doi: 10.1021/jp9917648.
29. Zhu J. Theoretical study of the optical absorption properties of Au–Ag bimetallic nanospheres. Physica E Low Dimens Syst Nanostruct. 2005;27(1-2):296-301. doi: 10.1016/j.physe.2004.12.006.
30. Pan ZW, Dai ZR, Wang ZL. Nanobelts of semiconducting oxides. Science. 2001;291(5510):1947-9. doi: 10.1126/science.1058120.
31. Tsaur BY, Lau SS, Mayer JW. Ion-beam-induced metastable phases in the Au–Co system. Philos Mag B. 1981;44(1):95-108. doi: 10.1080/01418638108222370.
32. Ajayan PM, Marks LD. Quasimelting and phases of small particles. Phys Rev Lett. 1988;60(7):585-7. doi: 10.1103/PhysRevLett.60.585.
33. Schaub R, Thostrup P, Lopez N, Laegsgaard E, Stensgaard I, Norskov JK, et al. Oxygen vacancies as active sites for water dissociation on rutile TiO(2)(110). Phys Rev Lett. 2001;87(26):266104. doi: 10.1103/PhysRevLett.87.266104.